

The Properties of Star-forming Regions within a Galaxy at Redshift 2

Mark Swinbank¹
 Alastair Edge¹
 Johan Richard¹
 Ian Smail¹
 Carlos De Breuck²
 Andreas Lundgren²
 Giorgio Siringo²
 Axel Weiss³
 Andrew Harris⁴
 Andrew Baker⁵
 Steve Longmore⁶
 Rob Ivison⁷

¹ Institute for Computational Cosmology,
 Department of Physics, University of
 Durham, United Kingdom

² ESO

³ Max-Planck-Institut für Radioastronomie,
 Bonn, Germany

⁴ Department of Astronomy, University of
 Maryland, College Park, USA

⁵ Department of Physics and Astronomy,
 Rutgers University, Piscataway, USA

⁶ Harvard-Smithsonian Center for Astro-
 physics, Cambridge, USA

⁷ United Kingdom Astronomy Technology
 Centre, Edinburgh, Scotland

The discovery and subsequent follow-up of one of the brightest sub-mm galaxies discovered so far is presented. First identified with the LABOCA instrument on APEX in May 2009, this galaxy lies at $z = 2.32$ and its brightness of 106 mJy at 870 μm is due to the gravitational magnification caused by a massive intervening galaxy cluster. Follow-up observations with APEX SABOCA have been used to constrain the far-infrared spectral energy distribution and hence measure the star formation rate, and Swedish Heterodyne Facility Instrument observations help constrain the excitation of the cold molecular gas. Furthermore, high resolution follow-up with the sub-mm array resolves the star-forming regions on scales of just 100 parsecs. These results allow study of galaxy formation and evolution at a level of detail never before possible and provide a glimpse of the exciting possibilities for future studies of galaxies at these early times, particularly with ALMA.

Massive galaxies in the early Universe have been shown to be forming stars at surprisingly high rates. The most prominent examples are sub-millimetre galaxies (SMGs) whose star formation rates can exceed $1000 M_{\odot} \text{ year}^{-1}$ (Chapman et al., 2003; Coppin et al., 2008). With this intense star formation rate, a massive galaxy (comparable to the stellar mass of a local elliptical galaxy) can be built in just 100 million years (Tacconi et al., 2008). As such, the sub-mm galaxy population may represent the formation epoch of today's massive elliptical galaxies (Lilly et al., 1999; Smail et al., 1997).

This is, however, a theoretically provocative conclusion as it is at odds with theoretical models. Indeed, sophisticated galaxy formation models have had to alter their prescriptions for starbursts radically, invoking exotic physics such as strong variations in the stellar initial mass function in order to account for the SMG population (Baugh et al., 2004). Although controversial, there is growing evidence that the increased interstellar medium (ISM) pressure within the warm, dense gas in local ultra-luminous infrared galaxies (ULIRGs) results in an increased Jeans mass (Perez-Torres et al., 2009). In order to test these controversial prescriptions, direct observational constraints on the properties of individual star-forming regions within high redshift galaxies are necessary. Such observations are technologically challenging, requiring the increased collecting area and sensitivity of the next generation telescopes, such as the Extremely Large Telescopes currently being planned and the Atacama Large Millimeter/Submillimeter Array (ALMA) under construction. Moreover, since the most intensely star-forming galaxies are also the most obscured, they are optically faint and difficult to identify and study on sub-kiloparsec (sub-kpc) scales.

Gravitational lensing

The most promising route for investigating the properties of high redshift galaxies on sub-kpc scales is to use massive galaxy clusters as natural lenses. Galaxy clusters magnify the images of distant galaxies that serendipitously lie behind them. This natural magnification causes

background galaxies to be strongly amplified and stretched, providing us with the opportunity of studying young and intrinsically faint galaxies with a spatial resolution that cannot be attained via conventional observations. The natural amplification caused by the galaxy cluster has two effects: (i) the image of the background galaxy is magnified at a fixed surface brightness (i.e. the total brightness is increased); and, (ii) the galaxy is not only amplified, but it is also stretched, making it possible to spatially resolve components of the galaxy from the ground.

LABOCA imaging of distant clusters

During recent Atacama Pathfinder Experiment (APEX) 870- μm observations of a massive galaxy cluster (MACS 2135-0102) we serendipitously discovered an extremely bright sub-mm galaxy with an 870- μm flux of 106 mJy (see Figure 1, left). This is three times brighter than any other known high-redshift star-forming galaxy and even brighter than the Cloverleaf and APM08279 quasars. Due to the high significance of the source, we were able to centroid the sub-mm emission to an accuracy of less than 0.5 arcseconds and identify the mid-infrared counterpart with a bright source detected by the Spitzer Space Telescope Infra-Red Array Camera (IRAC) and Multiband Imaging Photometer (MIPS); see Figure 1 right. Due to the brightness, we were able to obtain a redshift measurement for the galaxy of $z = 2.3259$ via the blind detection of CO(1–0) using the Zpectrometer on the Green Bank Telescope (GBT), confirming that the galaxy is high redshift and strongly gravitationally lensed. Indeed, using a detailed mass model of the galaxy cluster we derive an amplification factor of 32.5 ± 4.5 . Intrinsically therefore the 870- μm flux is ~ 3 mJy, typical of the sub-mm background, and, on account of the amplification, an ideal target for study. The CO(1–0) emission line flux can also be used to estimate the cold molecular gas mass; after correcting for lensing amplification we derive a gas mass of $2 \times 10^{10} M_{\odot}$.

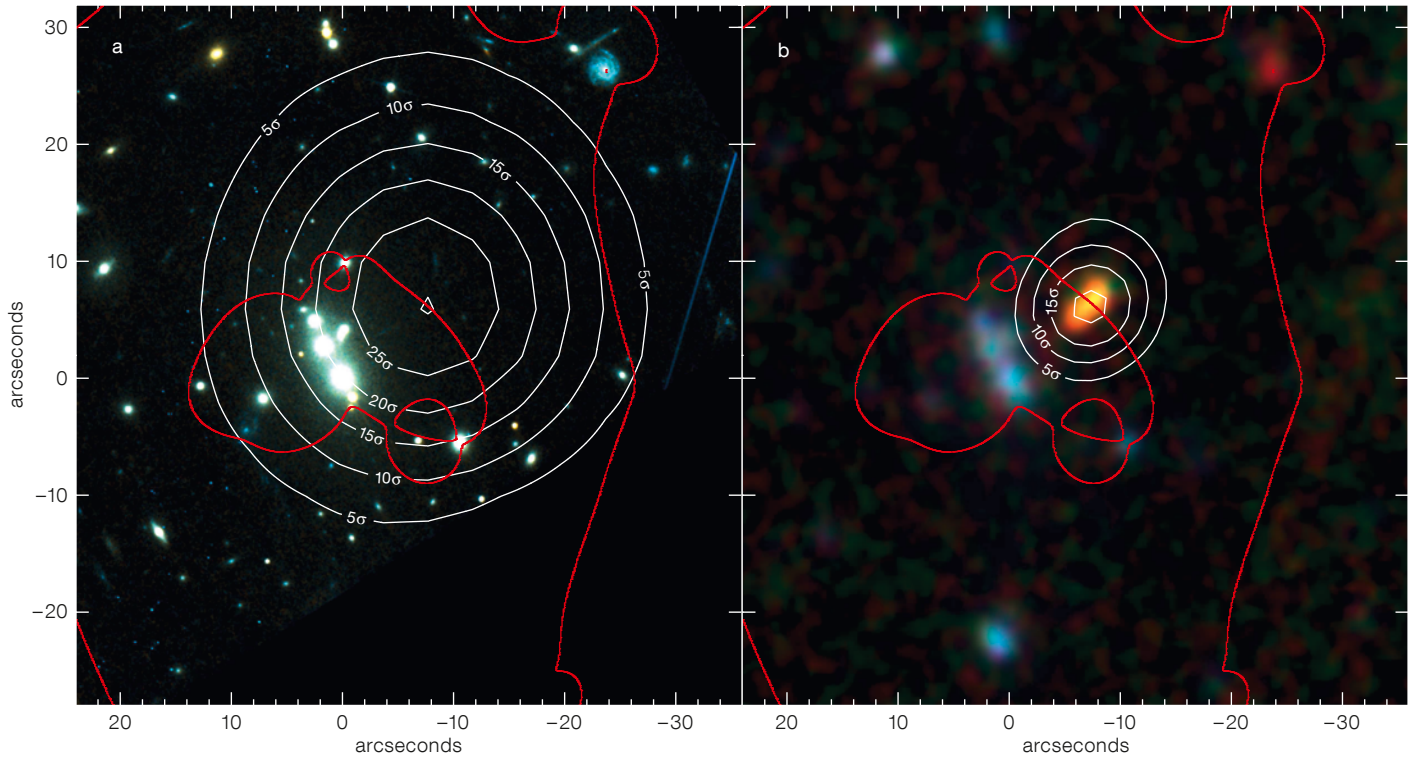


Figure 1. True colour HST VI-band image of the massive galaxy cluster MACSJ2135-0102 ($z_{cl} = 0.325$) is shown (left). The white contours denote the APEX/LABOCA 870- μm contours from the galaxy (contours denote 5, 10, 15, 20, 25, 30 σ), identifying an SMG with flux 106 mJy. The solid red lines denote the $z = 2.326$ radial and tangential critical curves from the best-fit lens model. The true colour IRAC 3.6, 4.5, 8.0- μm image of the cluster core is shown (right). The contours denote the intensity of the 350- μm map and show 5, 10, 15, 20 σ . The red lines again show the lens model critical curves.

SABOCA

With confirmation that this is a highly amplified background galaxy, observations at 350 μm using the SABOCA camera (see article by Siringo et al., p. 20) were carried out to parameterise the spectral energy distribution (SED); see Figure 2. With a measured 350- μm flux of 530 mJy we derive an intrinsic far-infrared luminosity of $1.2 \times 10^{12} L_{\odot}$. This suggests a star formation rate of 210 M_{\odot}/yr . If this star formation rate has been maintained, then it takes just ~ 120 Myr to build the observed stellar mass of $4 \times 10^{10} M_{\odot}$ and the remaining gas depletion timescale is a further 70 Myr. Together, this suggests that this intense star formation episode may be the first major growth phase of this galaxy.

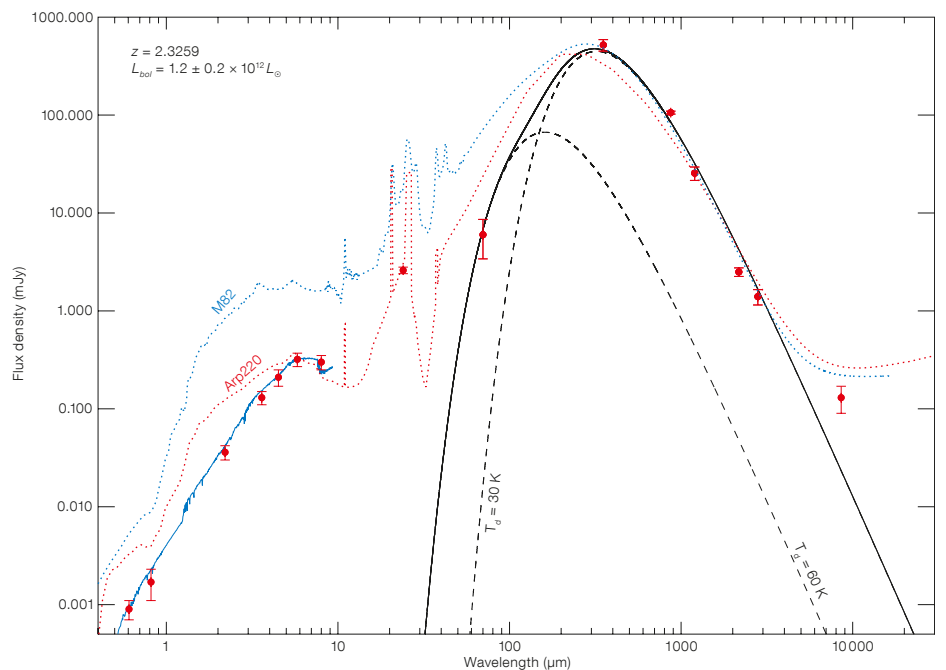


Figure 2. Spectral energy distribution (SED) of the lensed galaxy SMMJ2135-0102 is shown. To test how the SED of the galaxy compares to local starbursts, the SEDs of M82 (blue dashed line) and Arp220 (red dashed line), both arbitrarily scaled to the 1.2 mm flux, are overlaid. The solid black line

denotes the best fit modified blackbody to the photometry. Accounting for lensing amplification, the bolometric luminosity of the galaxy is $L_{bol} = 1.2 \pm 0.2 \times 10^{12} L_{\odot}$ which corresponds to a star formation rate of $\text{SFR} = 210 \pm 50 M_{\odot}/\text{yr}$.

Molecular gas properties

To further constrain the properties of the cold molecular gas, observations of the high- J CO emission (up to $J = 7$) were obtained with a combination of Institut de Radioastronomie Millimétrique Plateau de Bure Interferometer (IRAM PdBI; CO(3–2) up to CO(7–6)) and APEX Swedish Heterodyne Facility Instrument (SHFI) (CO(7–6)). In Figure 3a we show the CO(1–0) and CO(7–6) line profiles obtained with the IRAM Eight Mxer Receiver (EMIR) and APEX/SHFI respectively. All the CO spectra show multiple peaks that we decompose into a “red” component and a “blue” component which are separated by 300 ± 24 km/s. Since the ratio of the high/low- J emission lines reflects the excitation of the molecular gas, we extract and model the CO spectral line energy distribution (SLED) of both “red” and “blue” components using large velocity gradient (LVG) models (e.g., Weiss et al., 2005). Both components are best fit with two excitation models (with temperatures ~ 40 K and densities of approximately 10^3 and 10^4 cm $^{-3}$; see Figure 3b). The LVG modelling also includes the “equivalent size” of the CO-emitting region as a free parameter, and we are therefore able to estimate the size of each component indirectly. The SLED modelling suggests that both the “red” and “blue” components appear to have a compact core with radius ~ 150 pc surrounded by a more extended, diffuse region with radius ~ 500 pc. Although these equivalent sizes come with some uncertainty, the brightest CO-emitting regions appear similar to those seen locally as starbursts with a dense, active star-forming core surrounded by a diffuse gas disc, perhaps providing the first direct evidence for a diffuse disc in an SMG.

Resolving the star-forming regions

To resolve the sub-mm emission directly, Submillimeter Array (SMA) observations were used to image the galaxy’s 870- μ m (345 GHz) continuum emission with a 0.2-arcsecond synthesised beam and hence investigate the sub-mm morphology. The map resolves the galaxy into eight discrete components over ~ 4 arcseconds in projection (Figure 4). These components represent two mirror images

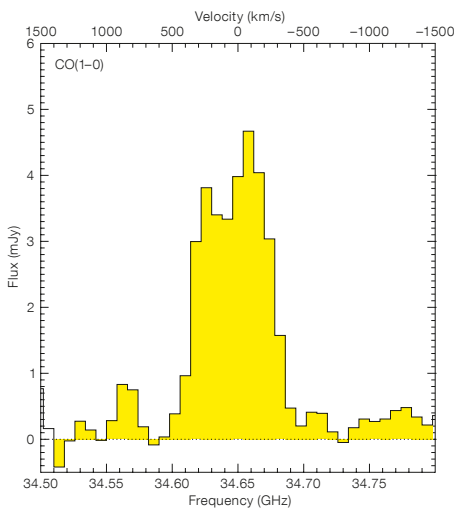


Figure 3a (above). Spectra of the $^{12}\text{CO}(1-0)$ and $^{12}\text{CO}(7-6)$ emission from SMMJ2135-0102 obtained with GBT/Zpec (left) and APEX/SFHI (right). The CO emission shows at least two velocity components separated by 300 km/s.

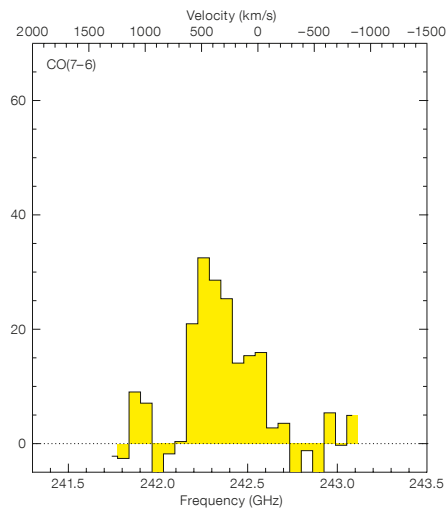
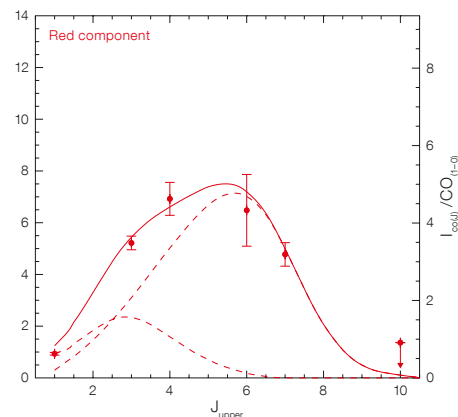
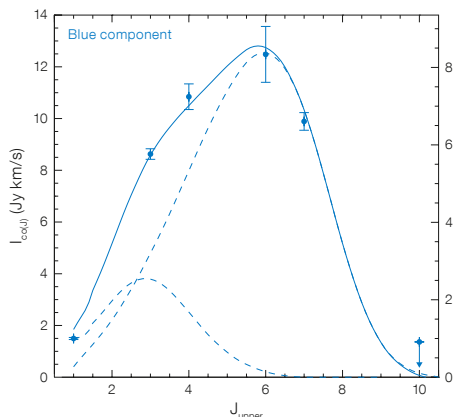


Figure 3b (below). The spectral line energy distributions (SLEDs) for the “blue” and “red” velocity components seen in CO emission.



of the galaxy each comprising four separate emission regions. Reconstructing the source-plane image using the lensing model, the galaxy comprises four bright star-forming regions in the source plane (indicated as A, B, C and D in Figure 4), that are separated by 1.5 kpc in projection. At the most highly amplified position, the source-plane resolution reaches ~ 90 pc which is comparable to the characteristic size of giant molecular clouds in the Milky Way (Scoville et al., 1989).

We compare the sizes and luminosities of the star-forming regions within SMMJ2135-0102 to giant molecular clouds (GMCs) in the local Universe (Scoville et al., 1989; Snell et al., 2002; Caldwell et al., 1996) in Figure 5. With-

in typical GMCs, constant energy density leads to a correlation between size and 260- μ m luminosity, such that luminosity is proportional to radius cubed. However, within the dense cores of GMCs and young HII regions, massive stars dominate the emission and produce luminosity densities a factor ~ 100 times higher than in typical GMCs (Hill et al., 2005) and shown by the upper dashed line in Figure 5. The star-forming regions within SMMJ2135-0102 are ~ 100 pc across, which is 100 times larger than dense GMC cores, but as Figure 5 shows their luminosities are approximately 100 times higher than expected for typical star-forming regions. Indeed, the luminosity densities of the star-forming regions within SMMJ2135-0102 are comparable

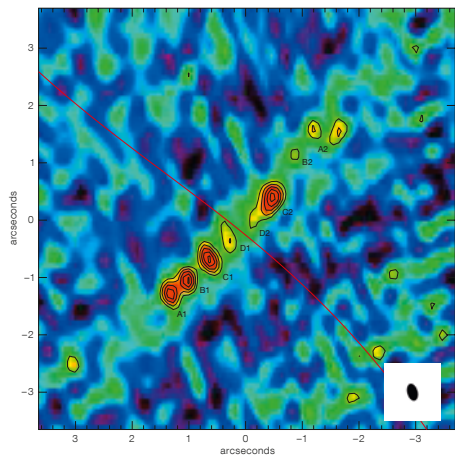


Figure 4a. The SMA map of SMMJ2135-0102 showing the image-plane morphology of the lensed galaxy at 870 μm . The galaxy comprises eight individual components, separated by up to 4 arcseconds in projection. The $z = 2.326$ radial critical curve (red line) is overlaid. The beam size is shown (lower right).

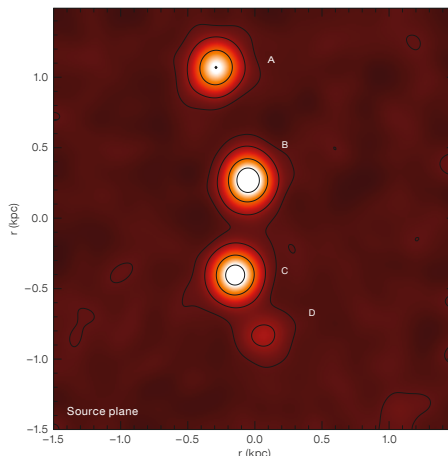


Figure 4b. The spatial distribution of the four components in the image plane from the lens model are shown. Each of the components (A, B, C and D), which are mirrored about the lensing critical curve, are identified.

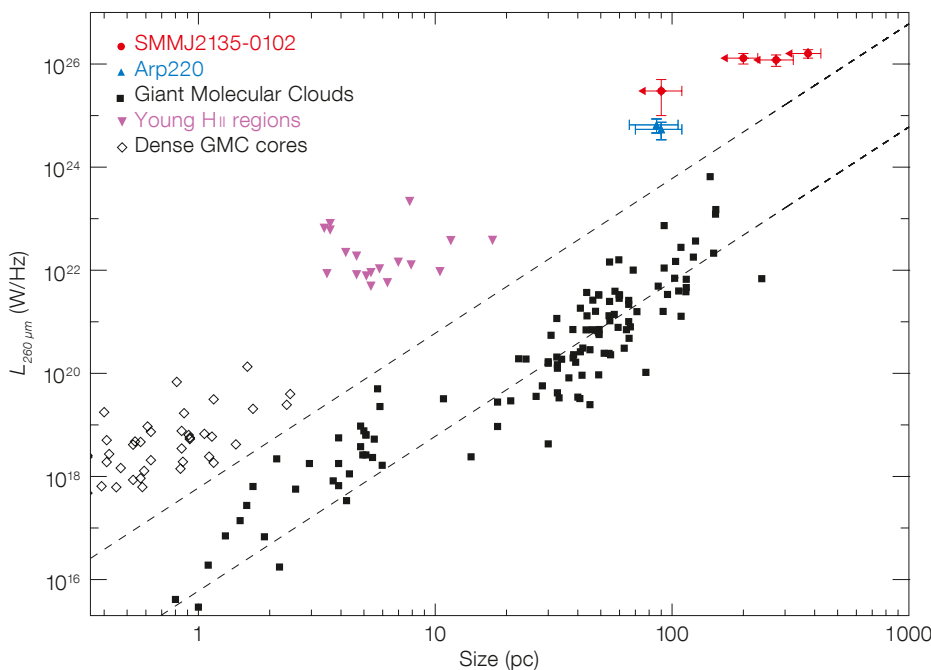


Figure 5. Correlation between size and luminosity for star-forming regions in SMMJ2135-0102 compared to those in the Milky Way and local galaxies. Black squares denote the size and 260- μm luminosities of giant molecular clouds in the Milky Way and the local group. The lower dashed line shows a fit to this relation (with slope fixed at $L_{260 \mu} \propto r^3$; i.e. constant energy density). The solid red points denote the sizes and luminosities of the star-forming regions in SMMJ2135-0102. The sizes and luminosities of dense cores of galactic GMCs in Henize 2-10 and M82 are plotted (open diamonds) as well as the two dominant star-forming regions within the local ultra-luminous infrared galaxy Arp220 (blue triangles).

to dense GMC cores, but with luminosities 10^7 times larger. Thus, it is likely that each of the star-forming regions in SMMJ2135-0102 comprises $\sim 10^7$ dense GMC cores.

The luminosity (and therefore star formation) density of the star-forming regions within SMMJ2135-0102 are also similar to those found in the highest density regions of the local starburst galaxy Arp220

(shown by blue triangles in Figure 5), although they are scaled up by a factor 10 in both size and luminosity (Sakamoto et al. 2008). Thus, the energetics of the star-forming regions within SMMJ2135-0102 are unlike anything found in the present-day Universe, yet the relations between size and luminosity are similar to local, dense GMC cores, suggesting that the underlying physics of the star-forming processes is similar. Overall, these results suggest that the recipes developed to understand star-forming processes in the Milky Way and local galaxies can be used to model the star formation processes in these high-redshift galaxies.

Outlook

Overall, these results provide unique insight into the physics of star formation within a galaxy at $z \sim 2$ on scales that would otherwise only be achieved with the increased light grasp and resolution of the next generation of facilities, such as ALMA. Indeed, due to the lensing effect we are able to provide an effective glimpse of two of the three science drivers for ALMA: to provide images at an angular resolution of 0.1 arcsecond of the dust continuum from distant galaxies; detect spectral CO emission in star-forming galaxies out $z = 3$ and measure their redshifts; albeit only for a single object. Thus, due to the fortuitous discovery with LABOCA and subsequent APEX/SHFI, SMA and GBT/Zpectrometer follow-up of this galaxy, we are able to provide unique insights into the key science that will be routine once ALMA reaches full science operations.

References

- Baugh, C. M. et al. 2004, MNRAS, 69, 3101
- Caldwell, D. A. et al. 1996, ApJ, 472, 611
- Chapman, S. C. et al. 2005, ApJ, 622, 772
- Coppin, K. E. K. et al. 2008, MNRAS, 384, 1597
- Hill, T. et al. 2005, MNRAS, 363, 405
- Lilly, S. et al. 1999, ApJ, 518, 641
- Livanou, E. et al. 2006, A&A, 451, 431
- Perez-Torres, M. A. et al. 2009, A&A, 507, L17
- Sakamoto, N. et al. 2008, ApJ, 684, 957
- Scoville, N. et al. 1989, ApJ, 339, 149
- Smill, I. et al. 1997, ApJL, 490, 5
- Snell, R. L. et al. 2002, ApJ, 578, 229
- Swinbank, A. M. et al. 2010, Nature (in press)
- Tacconi, L. et al. 2008, ApJ, 680, 246
- Weiss, A. et al. 2005, A&A, 440, 45

Further images in Press Release eso1012.